Decay channels of Al $L_{2,3}$ excitons and the absence of O K excitons in α-Al_2O_3

W. L. O'Brien, J. Jia, Q-Y. Dong, and T. A. Callcott
University of Tennessee, Knoxville, Tennessee 37996

D. L. Mueller and D. L. Ederer
National Institute of Standards and Technology, Gaithersburg, Maryland 20899

N. D. Shinn
Division 1114, Sandia National Laboratories, Albuquerque, New Mexico 87185

S. C. Woronick
Cornell University, Ithaca, New York 14850
(Received 24 June 1991)

The Al $L_{2,3}$ and O K thresholds for single-crystal α-Al_2O_3 have been studied by photoemission. Energy-distribution curves, constant-initial-state (CIS), and constant-final-state (CFS) spectra are reported and compared to the absorption spectrum reported previously. An exciton appears as a doublet at threshold in the Al $L_{2,3}$ CFS, CIS, and absorption spectra. The details of the Al $L_{2,3}$ CFS spectrum and absorption spectrum are similar, while the exciton is the only feature present in the CIS spectrum. Comparisons of the various Al $L_{2,3}$ spectra allow the probabilities of different exciton decay channels to be determined. The probability for nonradiative direct recombination of the exciton is found to be $(8\pm1)\%$ and the probability for Auger decay of the exciton is found to be $(72\pm20)\%$. Comparisons of the O K CIS and CFS spectra suggest that no O K exciton is formed.

INTRODUCTION

Conduction-band density of states are typically determined experimentally by measuring the absorption at energies near and above a core hole binding energy. A number of experimental techniques are available for measuring absorption spectra. In photoelectron techniques the energy dependence of the absorption is determined by monitoring either the decay of the core hole through Auger processes or the total secondary-electron yield as a function of the incident photon energy. In reflection techniques, the reflectivity is measured as a function of photon energy and converted into an absorption spectrum. In electron-energy-loss experiments, the energy loss of the incident electron beam is measured to give the absorption spectrum. For insulators, the presence of the core hole in the final state affects the absorption spectrum by the formation of core excitons. Core excitons appear near the absorption threshold and are often the main feature in the absorption spectrum.[1,2] This observation led to much debate in the early 1970s over whether the sharp intense features near threshold for alkali halide absorption were excitons or density-of-states features. The argument was resolved when Pantelides[1] used values for the energy gap of the alkali halides to show that these features lie within the band gap and were thus excitons.

Core excitons in alkali halides have been the subject of many investigations over the past few decades.[3-6] Particularly of relevance to this work is the work of Ichikawa and co-workers on the decay probabilities of Li (Ref. 5) and Na (Ref. 6) halides. Another group of insulators which exhibit intense core-exciton features at the absorption threshold are MgO, Al_2O_3, and SiO_2.[2] In this paper we present photoelectron spectroscopy results from single crystal α-Al_2O_3. Constant initial state (CIS) and energy distribution curves (EDC's) for the Al $L_{2,3}$ edge are used to determine the probability of two decay channels of the Al $L_{2,3}$ exciton with an analysis similar to that used by Ichikawa and co-workers for the Li (Ref. 5) and Na (Ref. 6) halides. Oxygen K CIS and constant-final-state (CFS) spectra yield no evidence for an O K exciton. We provide an argument to suggest why O K excitons may be suppressed.

EXPERIMENT

The experiment was performed on beamline U16 of the National Synchrotron Light Source, Brookhaven National Laboratory. The resolution of the extended range grasshopper monochromator used was 0.1 eV at the Al $L_{2,3}$ threshold and 1.5 eV at the O K threshold. Photoelectrons were detected with a double-pass cylindrical mirror analyzer. The sample used was a 1-mm-thick cut and polished single crystal of α-Al_2O_3. The sample was etched in 48% HF for a few minutes prior to vacuum insertion. This resulted in a carbon-free surface before bakeout. After bakeout small amounts of carbon contamination were removed by heating in 2×10^{-6}-Torr O_2 at 1050 °C for 5 min. The surface remained free of carbon contamination as measured by both Auger spectroscopy and valence-band photoemission for over 24 h. The

chamber pressure was 2×10^{-10} Torr.

To eliminate sample charging, a homemade electron flood gun with an extractor grid was employed. The flood gun was located 1.5 cm from the sample surface at grazing incidence. All the measurements reported in the present work were obtained with the flood gun operating at 3 V and delivering 4 μA. In this manner we observed no significant shift in the valence band as the photon energy was changed. Because of its use, however, binding energies are not referenced to the Fermi energy. The top of the valence band is therefore used as the reference for binding energies throughout this work. The photon flux was monitored with a clean copper grid. Examination of the flux measured in this manner showed no energy-dependent structure in the range of interest. All absorption measurements reported here are normalized by the photon flux.

DECAY CHANNELS OF EXCITONS

In a defect-free solid, a core exciton has four decay channels available if there are no states between the valence band and the core hole of interest. These four channels are represented schematically in Fig. 1. One possibility is that the exciton can decay by recombination and emit a valence electron in a process similar to Auger emission, Fig. 1(a). The final state of this process is identical to the final state in the normal valence-band photoemission and thus appears as an interference in the CIS spectrum if the valence band is chosen as the initial state. The exciton can also decay by an Auger process, involving two valence electrons, Fig. 1(b). Here the excited electron acts as a spectator during the decay. The other two channels involve photon emission. They are direct radiative recombination and radiative decay Figs. 1(c) and 1(d), respectively. For the radiative decay process, the excited electron acts as a spectator during the decay, similar to the Auger decay process.

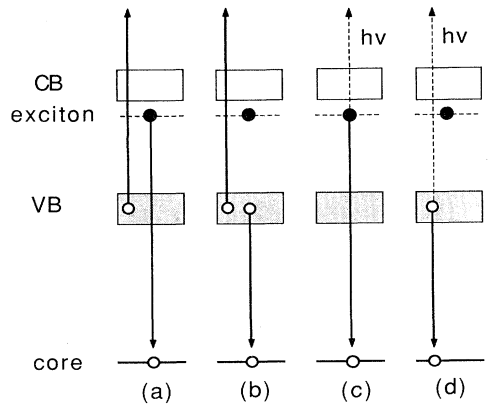

FIG. 1. Energy-level diagram showing conduction band (CB), valence band (VB), excited electron, and core hole. The exciton state is the core hole together with the excited electron. A core exciton has four decay channels available in a defect-free solid if there are no states between the excited core hole and the valence band. The exciton can recombine with (a) emission of a valence electron, (b) decay by an Auger process, (c) the emission of a photon, or (d) decay by valence-band x-ray emission.

The electronic structure of α-Al_2O_3 can be described as having an upper and lower valence band.[7,8] The upper valence band is formed primarily from O $2p$ states with some Al $3s$ states. The lower valence band is formed primarily from O $2s$ states with some Al $3s$ states. The next more tightly bound state is the Al $L_{2,3}$ core. Thus, if the upper and lower valence bands are considered together as the valence band, the Al $L_{2,3}$ core excitation has only four possible decay channels as described in Fig. 1. We will determine the decay probability of two of these channels, recombination and Auger decay [Figs. 1(a) and 1(b)]. To do this we examine the CIS spectrum and the EDC obtained with an excitation energy at the Al $L_{2,3}$ threshold.

The CIS spectrum is a result of quantum-mechanical interference between two processes, direct photoemission and recombination [Fig. 1(a)] of the exciton. These two processes do not simply add together to increase the intensity of the CIS emission. Instead they interfere with each other. The resulting line profile is asymmetric and requires the Fano formalism[9,10] for a proper description. It should be noted that CIS spectra are enhanced for localized excited states.[6] Electrons excited into the conduction-band states disperse and the excited electron will not be in the vicinity of the core hole throughout the core hole's entire lifetime. This reduces the conduction-band states contribution to CIS. Core excitons, however, are very localized. In fact, in lithium[5] and sodium[6] halides they are the only features observed in the CIS spectra because there is very little interaction between the valence band and the core levels for these compounds. In general, CIS spectra reveal the interference between several final-state channels and show enhancement due to localized absorption states. CFS spectra give a measure of the absorption due to excitation of the core electrons if Auger electrons are used as the final state. Since only one process is being measured there is no interference.

It is natural to separate the remainder of this paper into two parts, one describing the Al $L_{2,3}$ threshold and the other describing the O K threshold.

Al $L_{2,3}$ THRESHOLD

Energy distribution curves for α-Al_2O_3 are shown in Fig. 2 for various excitation energies near and above the Al $L_{2,3}$ threshold. The upper valence band peaks at around 3-eV binding energy and the lower valence band peaks at around 20-eV binding energy. We measure the width of the lower valence band to be 10.9 eV, in good agreement with published values.[11,12] The line shape of the upper valence band does not change over the range of photon energies studied here. At 78.6-eV excitation energy, the Al LMM Auger features, labeled P_1, P_2, and P_3 in Fig. 2, appear in the spectrum. These peaks have been assigned in Ref. 13. For the CIS spectrum we use the

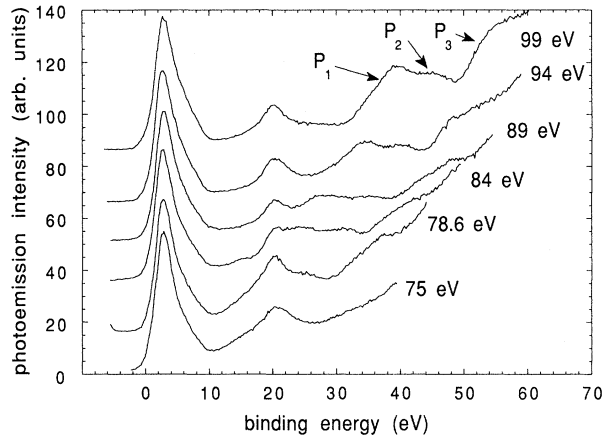

FIG. 2. Energy distribution curves for α-Al_2O_3 at excitation energies near the Al $L_{2,3}$ threshold. Features at binding energies near 3 and 20 eV are the upper and lower valence bands, respectively. The three Al *LMM* Auger peaks are designated P_1, P_2, and P_3. The upper valence band is used as the initial state in ClS and P_3 is used as the final state in CFS.

upper valence band as the initial state. For the CFS spectrum, we use the P_3 Auger electron, at kinetic energy of approximately 35 eV, as the final state. We will not analyze the behavior of the lower valence band in CIS or the Auger peaks P_1 and P_2 in CFS since P_1 and P_2 and the lower valence band coincide in kinetic energy near threshold and cannot be accurately separated.

The CFS spectrum is shown in Fig. 3 together with the absorption spectrum measured by soft-x-ray reflection spectroscopy.[2] The absorption spectrum is shifted by 0.3 eV to achieve the best match at threshold. We believe this shift is primarily due to different spectrometer calibrations. It can be seen that the features are nearly identical in position, although the relative intensities are somewhat different. The prominent doublet at threshold is the Al $L_{2,3}$ exciton. This doublet is shown on an expanded scale in Fig. 4 where the CFS and absorption spectra are compared to the CIS spectrum. The splitting of the peaks is 0.49 eV and the $I(L_3)/I(L_2)$ intensity ratio is 0.44 as measured from the absorption spectrum.[2] This nonstatistical ratio suggests that the exchange energy is similar to the spin-orbit energy and that intermediate coupling is required to interpret the spectrum.[2] By making this absorption measurement using photoelectron techniques, we have resolved the splitting of this exciton state. This observation implies that we have a well-prepared α-Al_2O_3 surface since other electron yield measurements,[12] which have failed to resolve the exciton splitting, were made with a resolution similar to those presented here. Also it should be mentioned that the absorption measurement presented in Figs. 3 and 4 is bulk sensitive since it was measured by reflectivity at near normal angle of incidence. The CFS spectrum is surface sensitive since the Auger electrons detected have a kinetic energy of about 35 eV. The absorption profiles of different phases of Al_2O_3 are known[14] to be distinct near threshold. Therefore we are certain that our crystal surface has not undergone any phase transition and that it is indeed stoichiometric α-Al_2O_3.

The only structure in the CIS spectrum occurs at the energy position of the exciton as shown in Fig. 4. Other spectral structure is not observed because the electrons in the valence band do not interact strongly with the core electrons. The asymmetric line shape is due to the interference between normal photoemission and the recombination channel [Fig. 1(a)]. The CIS spectrum is shown again in Fig. 5 with the background cross section included. The excitation appears as a small cross-section enhancement on the continuum background cross section. The variation of this background is due to the variation of the normal valence-band-photoemission cross

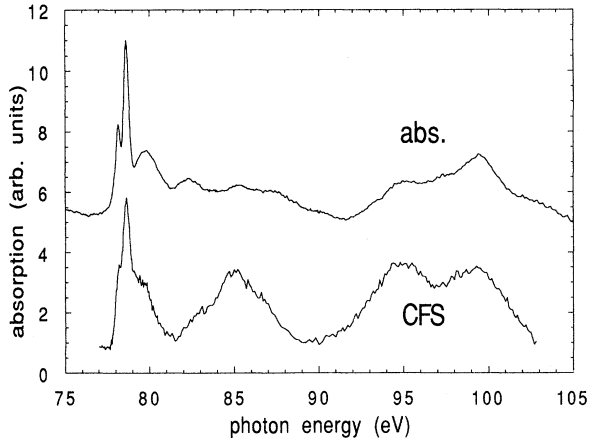

FIG. 3. Comparison of CFS spectrum with absorption spectrum. The absorption spectra were measured by soft-x-ray reflection spectroscopy (Ref. 2) and are bulk sensitive, while the CFS measurement is surface sensitive.

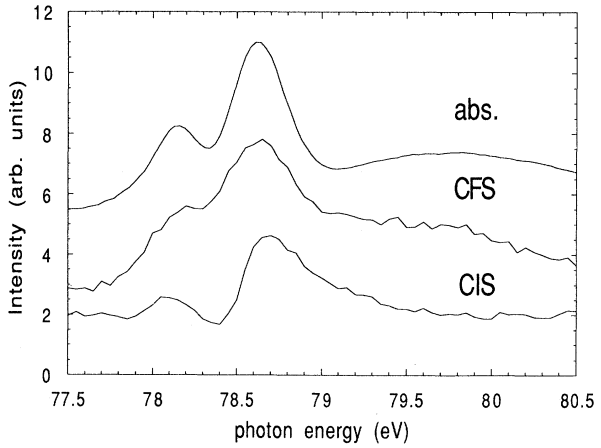

FIG. 4. Comparison of the CIS, CFS, and absorption spectra near threshold. Splitting of L_2-L_3 exciton is evident in each spectrum. No other structure appears in the CIS spectrum.

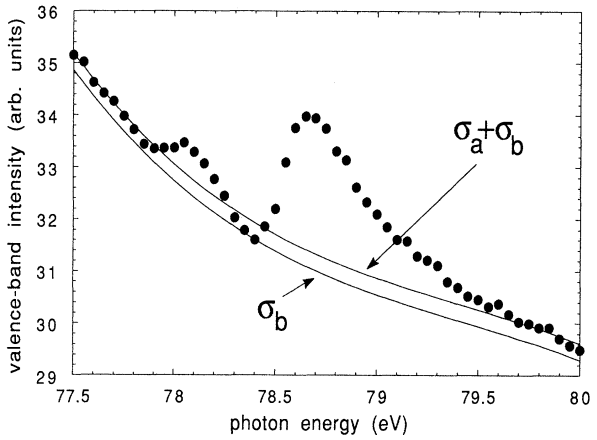

FIG. 5. CIS spectrum shown together with background. The background consists of two continua, one which interacts with the exciton state, σ_a, and one which does not, σ_b. The choice of these backgrounds was the largest source of uncertainty in the analysis of exciton decay probabilities.

section as the excitation energy is changed. Some of the variation is also due to the changing efficiency of the copper grid photon flux monitor.

The relative probability of exciton decay channels can be determined through analysis of the CIS and EDC spectra using the Fano formalism.[9,10] In the most basic representation of the Fano formalism one discrete state interacts with one continuum. Our spectrum involves two discrete states, each interacting with a different continuum. However, we feel that the uncertainty involved in our analysis do not justify the use of the more complicated formalism[10] with its many more unconstrained fitting parameters. Therefore we concentrate on the L_2 exciton and assume its interaction with the L_3 exciton is negligible. In the Fano formalism the ratio of the transition probabilities to the "modified" discrete state and to a band width $\pi\Gamma/2$ of unperturbed continuum states is

$$\frac{T}{(\sigma_a+\sigma_b)\pi\Gamma/2}=\frac{q^2\sigma_a}{(\sigma_a+\sigma_b)}\ , \tag{1}$$

where T is the transition probability to the modified discrete state (core exciton) and σ_a and σ_b represent two portions of the background cross section corresponding, respectively, to transitions which do and do not interact with the discrete state (see Fig. 5). The parameter q^2 is the ratio of peak height above and below the background, $\sigma_a+\sigma_b$ (Fig. 5), and the quantity Γ is a measure of the coupling between the discrete state and the continuum. The ratio of the recombination probability of the exciton to a $\pi\Gamma/2$ bandwidth of the valence-band cross section can be determined from the values of q^2, σ_a, and σ_b, obtained from the data in Fig. 5. We determine the value of this ratio to be 8%.

The ratio R of Auger decay probability to recombination probability is

$$R=S_A/S_D\ . \tag{2}$$

Here S_A is the integrated intensity of the Auger signal obtained from the EDC curve excited at 78.6 eV (resonant energy for the exciton) and S_D is the fraction of the valence-band intensity due to recombination. By comparing the integrated intensity of the three Auger peaks P_1, P_2, and P_3 to 8% (fraction produced by recombination) of the upper and lower valence-band intensity, we determine $S_A/S_D=9\pm1$ for the Al L_2 exciton. Since P_1 and P_2 and the lower valence band interfere at this excitation energy, we have determined intensity ratios for $P_3/(P_1+P_2+P_3)$ and the upper/lower valence band, from spectra obtained at higher excitation energies. These ratios are then used together with the measured intensities of P_3 and the upper valence band excited at 78.6 eV to obtain S_A/S_D.

The assumptions made in this analysis are that the intensity ratios of the Auger peaks P_1, P_2, and P_3 are the same at 78.6 eV as they are at higher energies and that the lower valence band changes in a manner similar to the upper valence band at threshold. To check these assumptions we have used a fourth-order polynomial fit to the background in a number of EDC's with excitation energies between 94 and 105 eV. From this analysis we find a constant $(P_1+P_2+P_3)/P_3$ intensity ratio of 3.5. Using this and assuming similar line shapes for the Auger peaks as at higher energies, we have determined the intensity ratio of the upper and lower valence band measured at 78.6 eV. This ratio is similar to those measured at higher energies. These comparisons give some confidence to the above approximations. It should be noted that for some compounds the Auger energy[6] and line shape[15] are different for excitation energies at threshold. Another assumption made in this analysis is that the 35-eV Auger electrons have the same escape depth as the 70-eV electrons of the upper valence band, which is not strictly correct but of negligible importance here.

An absolute value of the probability for the recombination channel, Fig. 1(a), can be determined by comparing the absorption spectrum to the CIS spectrum. The background below threshold in the absorption spectrum is due to direct excitations of the valence band. This statement is also true regarding the CIS spectrum. If the probability of the recombination channel was 100% the peak intensity to background ratio for the CIS spectrum and absorption spectrum would be identical. This ratio is smaller in the CIS spectrum since the probability of the exciton decaying by recombination is not 100%. The peak intensity to background ratio for the L_2 exciton in the absorption spectrum is 1.06. This is determined from fitting the exciton with a Lorentzian of full width at half maximum of 0.31 (Ref. [2]) and using a $0.31\pi/2$ bandwidth extrapolated background. This gives a value of 8% (8%/1.06) for the recombination probability and 72% ($9\times8\%$) for the Auger decay probability.

The largest uncertainty in using this technique is in the background selection for the CIS spectrum. By changing the constraints on the background fit we have estimated our error in decay probabilities at 15% due to this uncertainty. Thus we find a $(8\pm1)\%$ decay probability for the

recombination channel and a (72±20)% decay probability for the Auger channel. A similar estimate of the decay probabilities for the L_3 exciton produces similar results. In general, $L_{2,3}$ core holes in light-Z elements decay primarily by the Auger process and radiative decay is negligible. If this is also true for the exciton, the decay probabilities measured should add to 100% and that is what we find within the quoted uncertainty.

O K THRESHOLD

Energy distribution curves for α-Al_2O_3 are shown in Fig. 6 for excitation energies above the O K threshold. The small features at 3- and 20-eV binding energies are the upper and lower valence bands, respectively. The intensity of these features is weak due to their low cross sections at these photon energies. The peak near 70-eV binding energy is the unresolved Al $L_{2,3}$ cores states. Three O KLL Auger peaks appear in the EDC. We identify these peaks as the $OKL_{2,3}L_{2,3}$, O $KL_1L_{2,3}$, and OKL_1L_1 for P_1, P_2, and P_3, respectively. This assignment is based on the observation that the Auger peaks are approximately evenly spaced with a separation equal to the upper and lower valence-band separation. For the CIS spectrum we use the upper valence band as the initial state. For the CFS spectrum we use the P_2 Auger peak. These spectra are shown in Fig. 7.

There is no obvious enhancement at threshold in the O K CIS spectrum relative to the O K CFS spectrum. This is in contrast to what is observed at the Al $L_{2,3}$ threshold. The details of the CIS and CFS spectra are different, however, and the threshold for the CIS spectrum is a volt higher than for the CFS spectrum. The difference in the thresholds may be due to the effects of interference inherent in CIS spectra. The peak height to background ratio in the CIS spectrum is 25%. This large increase is due primarily to the small cross section for direct photoemission from the valence band at these energies. In fact, if the cross section of normal valence-band photoemission is assumed to follow E^{-3}, the intensity of the features in the O K CIS are 90 times less intense than the features in the Al $L_{2,3}$ CIS spectrum.

The lack of enhancement at the O K threshold in the CIS spectrum relative to the CFS spectrum suggests that no O K exciton is formed. A possible explanation of why the Al $L_{2,3}$ exciton forms while the O K exciton does not can be made by assuming α-Al_2O_3 to be purely ionic. The Al L_2 exciton in α-Al_2O_3 is within 1.0 eV of the $2p^6 \rightarrow 2p^6 3s^1$ transition for the Al^{3+} ion.[2] This suggests that the $L_{2,3}$ exciton is formed from an Al $3s$ level pulled down into the band gap from the bottom of the conduction band by the core hole potential.[2] The lowest-lying allowed K excitation for the O^{2-} ion is the $1s^2 2s^2 2p^6 \rightarrow 1s^1 2s^2 2p^6 3p^1$ transition. These levels are further up in the conduction band than the Al $3s$ level and would therefore need to be pulled down further to form an exciton in the band gap.

Furthermore, the O K core hole potential is screened by the additional $2p$ electrons associated with O^{2-}, while there are no valence electrons present on Al^{3+} to screen the Al $L_{2,3}$ core hole potential. The screening of the O K core hole potential reduces its effect on conduction-band levels. Both these effects, screening and position of levels near the conduction-band minimum, suggest that an Al $L_{2,3}$ exciton is more likely to form than an O K exciton. Recent self-consistent-field band-structure calculations[8] have shown that α-Al_2O_3 is highly ionic, supporting the use of this explanation.

SUMMARY

In summary we have measured EDC, CIS, and CFS spectra near and above the Al $L_{2,3}$ and O K thresholds

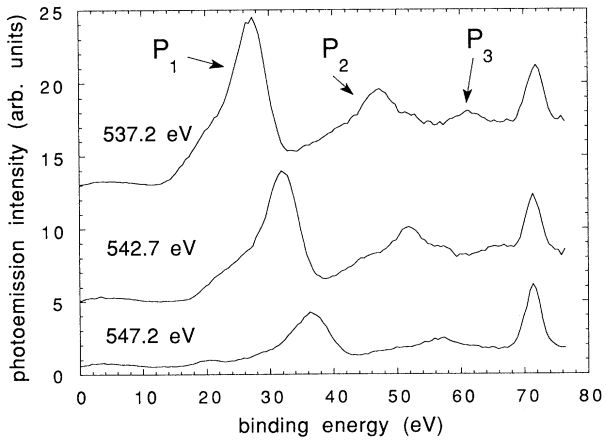

FIG. 6. Energy distribution curves of α-Al_2O_3 with excitation energies near the O K threshold. The features at binding energies near 3, 20, and 72 eV are the upper valence band, lower valence band, and Al $L_{2,3}$ core state, respectively. The three O KLL Auger peaks are designated P_1, P_2, and P_3. The upper valence band is used as the initial state for CIS and P_2 is used as the final state for CFS.

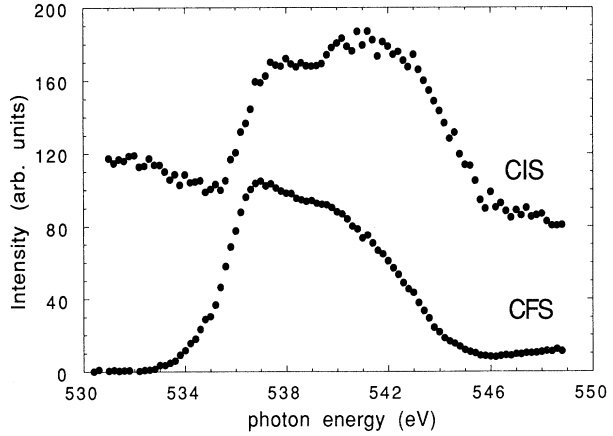

FIG. 7. Comparison of O K CIS and CFS spectra. The lack of a distinct feature near threshold in the CIS spectrum compared to the CFS spectrum suggests that no O K exciton is formed.

on single-crystal α-Al_2O_3. Sample charging was effectively eliminated through use of an electron flood gun. The Al $L_{2,3}$ CFS spectrum is similar to the absorption spectrum with the core exciton appearing as an intense doublet at threshold. Decay probabilities for two of the four Al $L_{2,3}$ exciton decay channels were determined from the CIS and EDC spectra. The exciton is 9 ± 1 times more likely to decay by the Auger channel as by direct recombination. Comparisons of the O K CIS and CFS spectra suggest that no O K exciton is formed. This is consistent with an explanation based on core hole screening and the relative positions of conduction-band states.

ACKNOWLEDGMENTS

This work was supported by the National Science Foundation, Grant No. NSF-DMR-8715430, and the National Institute of Standards and Technology. This work was carried out at the National Synchrotron Light Source, which is supported by the U.S. Department of Energy Under Contract No. DE-AC02-76CH00016.

[1]S. T. Pantelides, Phys. Rev. B **11**, 2391 (1975).
[2]W. L. O'Brien, J. J. Jia, T. A. Callcott, J.-E. Ruebensson, D. L. Mueller, and D. L. Ederer, Phys. Rev. B **44**, 1013 (1991).
[3]E. T. Arakawa and M. W. Williams, Phys. Rev. Lett. **36**, 333 (1976).
[4]F. Sette, B. Sinkovic, Y. J. Ma, and C. T. Chen, Phys. Rev. B **39**, 1125 (1988).
[5]K. Ichikawa, M. Kamada, O. Aita, and K. Tsutsumi, Phys. Rev. B **32**, 8239 (1985).
[6]M. Kamada, O. Aita, K. Ichikawa, and K. Tsutsumi, Phys. Rev. B **36**, 4962 (1987).
[7]I. P. Barta, J. Phys. C **15**, 5399 (1982).
[8]Y-N. Xu and W. Y. Ching, Phys. Rev. B **43**, 4461 (1990).
[9]U. Fano, Phys. Rev. **124**, 1866 (1961).
[10]U. Fano and J. W. Cooper, Phys. Rev. **137**, A1364 (1965).
[11]S. P. Kowalczyk, F. R. McFeely, L. Ley, V. T. Gritsyna, and D. A. Shirley, Solid State Commun. **23**, 161 (1977).
[12]I. A. Broytov and Y. N. Romashchenko, Fiz. Tverd. Tela (Leningrad) **20**, 664 (1978) [Sov. Phys. Solid State **20**, 384 (1978)].
[13]P. H. Citrin, J. E. Rowe, and S. B. Christman, Phys. Rev. B **14**, 2642 (1976).
[14]A. Balzarotti, F. Antonangeli, R. Girlanda, and G. Martino, Solid State Commun. **44**, 275 (1982).
[15]T. Tiedje, K. M. Colbow, D. Rogers, and W. Eberhardt, Phys. Rev. Lett. **65**, 1243 (1990).